Hindawi Publishing Corporation
EURASIP Journal on Wireless Communications and Networking
Volume 2007, Article ID 63503, 14 pages
doi:10.1155/2007/63503

Research Article

Grey Target Tracking and Self-Healing on Vehicular Sensor Networks

Yih-Fuh Wang[1] and Lin-Lin Liu[2]

[1] *Department of Computer Science and Information Management, Leader University, No. 188 Sec. 5 Anjhong Rd., Tainan 709 , Taiwan*
[2] *Institute of Applied Information, Leader University, No. 188 Sec. 5 Anjhong Rd., Tainan 709 , Taiwan*

Received 3 October 2006; Revised 30 January 2007; Accepted 6 April 2007

Recommended by Biao Chen

The wireless vehicular sensor network (VSN) has been very useful for many transportation application systems, but it does not operate like the traditional wireless sensor network. For safety reason, the vehicle-vehicle and vehicle-gateway communication modes must be stable. The motion of the vehicle, the environment of the roads, and other uncertain traffic conditions all pose challenges to the system. Therefore, how to keep link stability becomes an important issue. In this paper, we propose a scheme that uses *grey target tracking* to self-heal or reroute in advance the weak link on an alternative route as failure occurs and makes the whole vehicular sensor network more stable. Although this scheme increases the average latency and control overhead, it supports higher survivability and effective reflections on rerouting.

1. INTRODUCTION

The wireless vehicular sensor network (VSN) has been widely investigated and proved to be very useful for traffic pattern analysis, road surface diagnosis, urban environmental monitoring, or street-level air pollution monitoring [1]. Unlike the traditional wireless sensor network (WSN), VSN is composed of hundreds or thousands of low-cost, low-power, multifunctional, and small sensors [2, 3]. The VSN has high computational power, provides high storage space, and has enough energy in mobile sensor nodes. In practice, it is mainly employed for supporting car safety, such as exchanging safety-relevant information or remote diagnostics using data from sensors built into vehicles, and mobile Internet access.

In a VSN, each vehicle is responsible for sensing one or more events, routing messages to other vehicles or roadside base stations, and processing sensed data. As shown in Figure 1, there are some moving vehicles and communication devices serving as base stations installed along the roads. For that, car safety can be protected by early broadcasting to police or neighbor cars as accidents occur. Then, a VSN is also able to forward these accident information related to car condition directly to roadside base stations or distant police or emergency centers so that they can make necessary emergency response and medical treatment decisions as soon as possible [4]. Moreover, the roadside base stations broadcast or multicast it to neighbor cars to avoid more accidents.

The VSN can be used in many cost-effective ways [4, 5] to gather traffic information to better understand how traffic knots, and point out the situation in order to reduce congestion, minimize emission, decrease fuel consumption, or foster traffic security. How vehicular ad hoc network (VANET) built VSN by equipping vehicles with onboard sensor devices has been introduced by [4, 5] (see Figure 1). The solution for car safety communication in VSN is to use intervehicle communication (IVC) [6]. As the vehicles move along the road, the propagation of the information should follow the same one-dimensional movement. Another difference is related to the fact that in case of IVC, all vehicles are moving and their relative speed with respect to each other is very small, resulting in stable wireless links between vehicles. US FCC has allocated a block of spectrum from 5.85 to 5.925 GHz band for IVC and vehicle-to-road communications (VRCs) that can support a wide range of applications [7]. One combined vehicular communication [7] is built with IVC, cellular

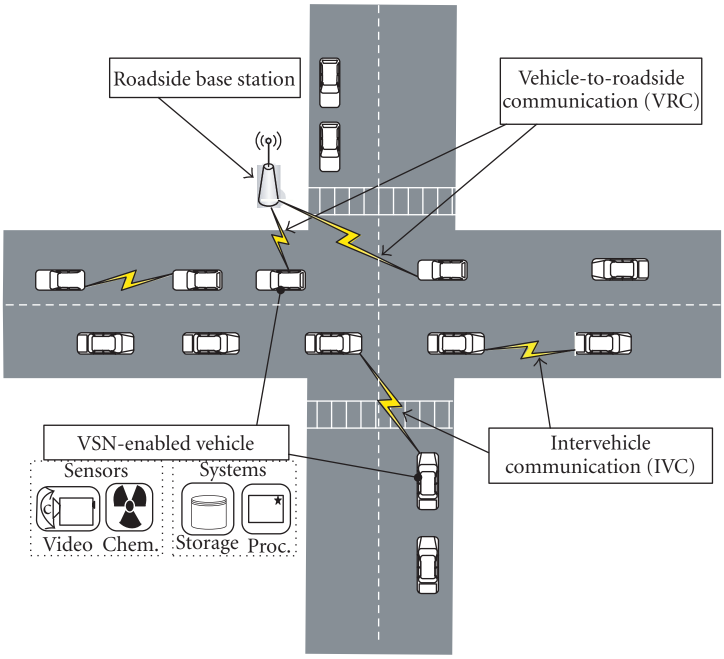

Figure 1: Vehicular sensor networks.

networks, and satellite networks (see Figure 2). Unlike IVC, vehicular communication enables necessary information to be uploaded and downloaded independently of space headway which is the space between moving vehicles, ships, or targets.

Since vehicles travel at a higher speed, [8] designs a vehicular mesh (VMesh) network, which is an ad-hoc network or a traditional wireless sensor network with no centralized authority or infrastructure, to accomplish reliable data transit. In this scheme, mobile nodes can move, be added, or be deleted as the network realigns itself. One of the benefits of a mesh network is that it has the abilities of self-forming, self-healing, and self-balancing. As shown in Figure 3, one of the applications of using VMesh as a transit network is to establish connections between disjoint sensor networks.

Nowadays, the rapid deployment of network infrastructures in various environments triggers new applications and services that in turn generate new constraints. For example, heterogeneous networks will integrate ad hoc and sensor solutions into wired and/or wireless fixed infrastructures in future. The integration of ad hoc and sensor networks with the Internet and wireless infrastructure networks increases network capacity, coverage area, and application domains. In this paper, we attempt to combine these heterogeneous networks with vehicular sensor networks (VSNs), vehicular mesh networks (Vmeshs), and other existing networks. While the interconnection of these networks must ensure transport traffic between a source and a destination, it must also keep on providing service of a very high quality and make various flows safe and secure. Carrying out these challenges requires the modification and/or the adaptation of some protocols.

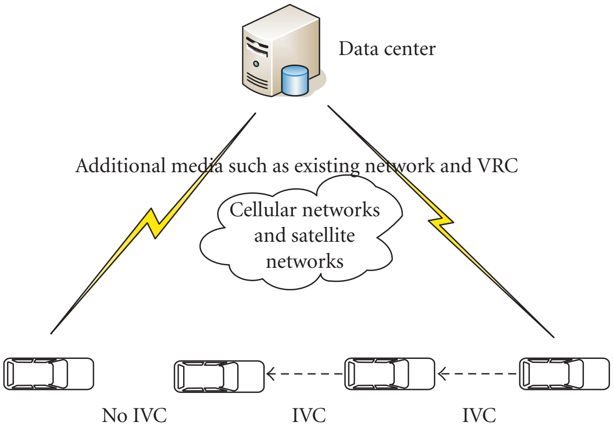
Data center
Additional media such as existing network and VRC
Cellular networks and satellite networks
No IVC
IVC
IVC

Figure 2: A combined network.

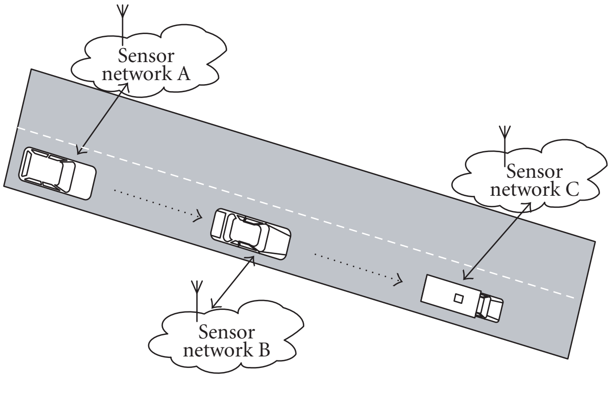

Figure 3: Using VMesh to connect disjoint sensor networks.

For safer and more reliable data transmission on VSN, ensuring more stable and robust communication link is more important than saving energy and decreasing communication costs, especially for emergency relief service in police centers and traffic control. Therefore, we propose a simple target-tracking algorithm that detects and tracks moving vehicles, and alerts them when they move beyond the safety range. The moving target-tracking scheme is broadly applied in many areas, such as aeronautical systems, antimissile, satellite manipulation, videoconferencing, and autonomous mobile robots [9, 10]. In addition to the sensory detection module [6], there are two major issues in a general position-based tracking system. One is the estimation/prediction of the target position from noisy sensory measurements and the other is the motion control of the tracker to track the moving target.

For some vehicles or fast movable ad hoc sensor networks, the mobility on VSN may frequently result in link failure. The failure protection becomes an essential challenge. Since sensor malfunction is caused by broken links or weak links, the system builds up protection and rerouting or self-healing scheme to avoid link failure of networks. However, as multiple sinks or cluster head paths build in a VSN, either simple or single link broken will cause tremendous damage to the working and maintenance of the VSN. Meanwhile, it is necessary to enhance the system prediction capability to avoid frequent failure for moving vehicles.

Greater mobility increases the volume of controlled traffic required to maintain broken routes. Some crucial on-demand mechanisms for minimizing broken links are provided to ensure rerouting responsiveness and efficiency on on-demand manner [11, 12]. Because each vehicle moves with different mobilities, the links are thus unstable or weak. Since topology has changed fast and frequently on wireless vehicular sensor networks, this motivates us to develop a scheme for preventing or reducing network errors. In this paper, we propose and investigate a *grey target-tracking resilient routing* (GTTRR) protocol for vehicular sensor networks to prevent network failure caused by failed or weak links. We apply a grey target-tracking strategy to track the moving target and self-heal or reroute in advance some weak links before link failure occurs. It makes routing decision with grey predict system [13, 14] because the grey system only needs a few data to perform tracking with high accuracy. It is very suitable for real-time processing requirement. The simulation of the proposed scheme shows that the links become more reliable since rerouting strategy starts before any network link becomes weaker. In this paper, Section 2 presents the target tracking with grey system. Section 3 shows the simulation model and the results. Finally, a conclusion is given.

2. GREY TARGET-TRACKING RESILIENT ROUTING

If the sensor in the vehicle has a fast response time, it is possible to estimate the current pose of the vehicle and to support real-time tracking performance. On the contrary, if the sensor has a slow response time, the estimation is no longer sufficient for a real-time tracking system [15]. For these reasons, many tracking systems use intelligent strategies to predict the potential position of the object ahead at the next time period. The predicted result serves two purposes [10], one is for the object (target) detection module to speed up the detection using inverse coordinate transformation, and the other is for the motion control module to decide motion parameters. Once the accurate pose of object has been predicted, the tracking system can then be performed. In a robot soccer game, the controller of the visual tracking system usually monitors the pan and tilt angular velocities of the platform to which a camera is attached; and for autonomous mobile robots, the driving and steering velocities are employed to follow a moving object (moving ball in a robot soccer game).

Most of the existing approaches to target tracking need a prior dynamics model of target for prediction. In many cases, the addition of the exact dynamic models is either difficult to obtain or needs complex mathematical descriptions, such as a walking human and robot soccer games [9]. Some algorithms proposed for target position predictions involve calculating the position, velocity, and acceleration of the moving targets from sensory measurements. The target motion trend can be predicted according to a polynomial description that fits the past trajectory [15, 16]. Owing to the sensor characteristics and the sampling rate of digital information, the measured target trajectory data are usually not accurate enough for prediction purpose. Therefore, a prior tracking scheme using grey prediction to deal with the problem of dynamic and complex computation was proposed in this paper.

In a VSN, the wireless vehicles can configure themselves to form a communication infrastructure so that sensed data can be transmitted across the vehicles hop by hop. After the mission of a sensor node is updated, it monitors the interest of user and reports data when an interesting phenomenon appears. We term a sensor node that has data to report as the *source* and those that collect data as *sinks* [6, 12]. A sink collects reported information and sends it back to the user. The sink node functions like a cell center, cluster head, gateway, or base station.

Sometimes the sink broadcasts (one-to-many) the interests to all sensor nodes in the network. Each sensor node stores the interest in a local cache and uses the gradient fields within the interest descriptors to identify the most suitable path to the sink. These paths are then used by source nodes to communicate the sensed data to the sink [12, 17] like a structure of *multicast trees*. In VSN, multicast trees with memberships, joints, and leaves are likely to be frequently occurring, especially for situations when the group is short-lived for distribution of a query or a short notification. Moreover, a more frequent occurrence is actually the opposite problem, clustering (many-to-one) communication, when several sources of data stream to the same sink [12].

2.1. Grey system

Our proposed scheme applies the grey system to target tracking on VSN. The grey system was created and developed by Deng in 1988 [13], and the most amazing aspect of the grey theory is that the estimation is still valid under high

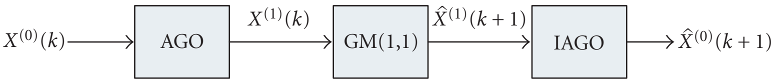

Figure 4: The procedure of simple grey prediction.

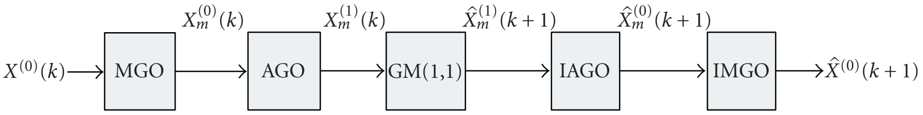

Figure 5: The procedure of grey prediction with MGO.

uncertainty with only limited sampled data [13] (only four data). The grey theory is developed from the grey exponential law. The procedures of the GM(1,1) model, AGO, and MGO are described in detail in the appendix.

Simply, we can present the entire procedure as

$$\begin{aligned}&\hat{x}(0) = \text{IAGO} \bullet \text{GM}(1,1) \bullet \text{AGO} \bullet x(0),\\&x(0) : \text{raw data sequence,}\\&\hat{x}(0) : \text{predictive data sequence.}\end{aligned} \tag{1}$$

A predicted value can be obtained by inverse transform. The accuracy of such a prediction certainly depends on the characteristics of the system [13]. If we have used MGO, we have to use another presentation as follows:

$$\hat{x}(0) = \text{IMGO} \bullet \text{IAGO} \bullet \text{GM}(1,1) \bullet \text{AGO} \bullet \text{MGO} \bullet x(0). \tag{2}$$

In particular, grey prediction accepts that the internal structure, parameters, and characteristics of the observed system are unknown. When making grey prediction, it is not clear to find the trend of a nonnegative sequence with arbitrary distribution. However, if we accumulate the sequence, we will get a monotonically nondecreasing sequence. Then, with the grey exponential law, an optimum exponential curve can be obtained to fit this sequence. The block diagram of a grey predictor is shown in Figures 4 and 5. The flowchart of grey model construction is shown in Figure 6.

2.2. Tracking moving target

A simple algorithm that detects and tracks a moving target and alerts sensor nodes along the projected path of the target is developed in [18]. The algorithm involves only simple computation and localizes communication only to the nodes in the vicinity of the target and its projected course. In order to be energy efficient, the system must leverage data processing and decision-making ability inside the network as much as possible. This is because with today's technology, the power budget for communication is many times more than that for computation. The goal is to track and predict the movement of an appropriate target and alert the sensors that are close to the predicted path of the target. The target can be a moving vehicle, for example, or can be a phenomenon such as an approaching fire. It is assumed that each individual sensor node (cluster head) is equipped with appropriate sensory device(s) to be able to detect the target as well as to estimate its distance from the sensed data. The sensors (cluster heads) that are triggered by the target collaborate to localize the target in the physical space to predict its course. Tracking a target involves three distinct steps [18] described as follows:

(1) detecting the presence of target,

(2) determining the direction of motion of target,

(3) alerting appropriate nodes in the network.

In this paper, we employ the grey prediction system to replace estimation in the tracking step and improve the function of data transmission in the alerting step. The most amazing aspect of the grey theory is that the estimation is still valid under high uncertainty with only limited sampled data (only four data). Predicting the location of the object (vehicle) is a common mean for tracking a moving object (vehicle). Grey prediction assumes that the internal structure, parameters, and characteristics of the observed system are unknown. It attempts to establish a grey model from the recent historical measurements of the external motion (the value of the last four data) for obtaining the predicted value.

In tracking steps, grey prediction will decrease the times required for estimation because linear regression need not be performed. In alerting step, we send *warning* message when moving targets (vehicles) move out of the transmission threshold or when the link between vehicle-vehicle or vehicle-cluster head is weak, and protect the weak link by rerouting in advance.

The process of the path discovery [19, 20] is initiated whenever a source node (vehicle) needs to communicate with another node or link weakness is sensed for which it has no routing information in its table. Every sensor node maintains two separate counters: a node sequence number and a broadcast id. The source node initiates path discovery by broadcasting a route request (RREQ) packet to its neighbors [19, 20].

Most reactive routing protocols, such as AODV and DSR, have similar route discovery mechanisms [19, 20]. In this paper, we adopt a similar route discovery method. Figure 7 shows an example of route discovery [19, 20], in which a

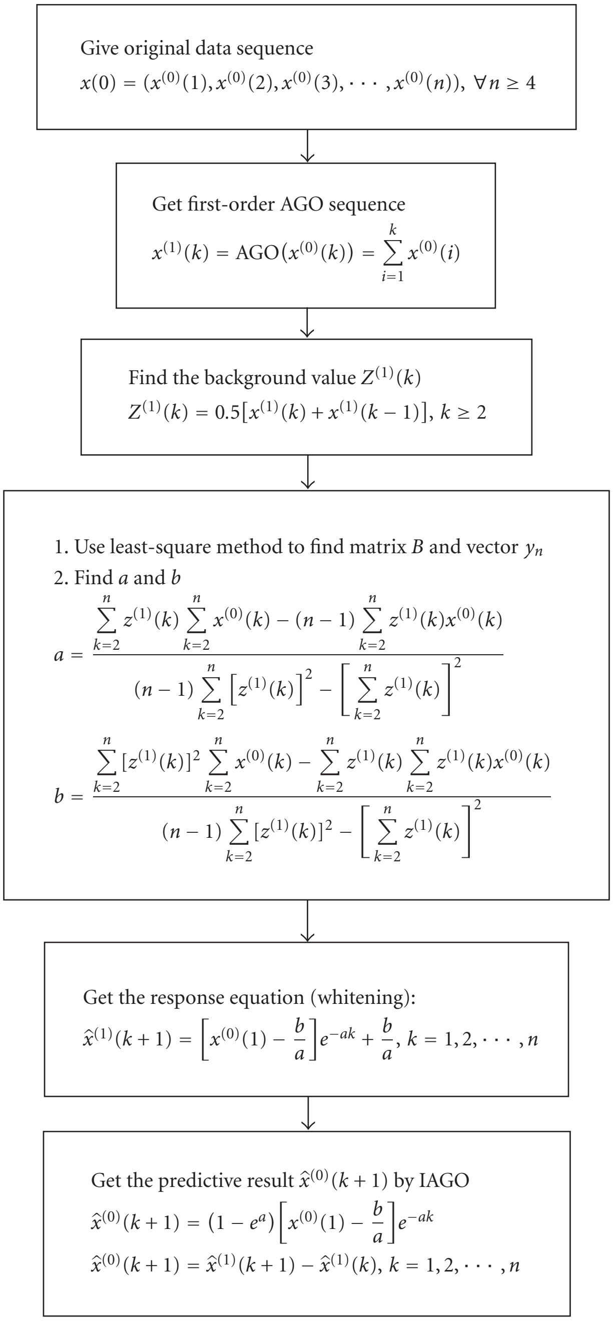
Give original data sequence
$x(0) = (x^{(0)}(1), x^{(0)}(2), x^{(0)}(3), \cdots, x^{(0)}(n)),\ \forall n \geq 4$
Get first-order AGO sequence
$x^{(1)}(k) = \mathrm{AGO}(x^{(0)}(k)) = \sum_{i=1}^{k} x^{(0)}(i)$
Find the background value $Z^{(1)}(k)$
$Z^{(1)}(k) = 0.5[x^{(1)}(k) + x^{(1)}(k-1)],\ k \geq 2$
1. Use least-square method to find matrix B and vector y_n
2. Find a and b
$a = \dfrac{\sum_{k=2}^{n} z^{(1)}(k) \sum_{k=2}^{n} x^{(0)}(k) - (n-1) \sum_{k=2}^{n} z^{(1)}(k) x^{(0)}(k)}{(n-1) \sum_{k=2}^{n} \left[z^{(1)}(k)\right]^2 - \left[\sum_{k=2}^{n} z^{(1)}(k)\right]^2}$
$b = \dfrac{\sum_{k=2}^{n} [z^{(1)}(k)]^2 \sum_{k=2}^{n} x^{(0)}(k) - \sum_{k=2}^{n} z^{(1)}(k) \sum_{k=2}^{n} z^{(1)}(k) x^{(0)}(k)}{(n-1) \sum_{k=2}^{n} [z^{(1)}(k)]^2 - \left[\sum_{k=2}^{n} z^{(1)}(k)\right]^2}$
Get the response equation (whitening):
$\hat{x}^{(1)}(k+1) = \left[x^{(0)}(1) - \frac{b}{a}\right] e^{-ak} + \frac{b}{a},\ k = 1, 2, \cdots, n$
Get the predictive result $\hat{x}^{(0)}(k+1)$ by IAGO
$\hat{x}^{(0)}(k+1) = (1 - e^{a}) \left[x^{(0)}(1) - \frac{b}{a}\right] e^{-ak}$
$\hat{x}^{(0)}(k+1) = \hat{x}^{(1)}(k+1) - \hat{x}^{(1)}(k),\ k = 1, 2, \cdots, n$

Figure 6: The flowchart of grey model construction.

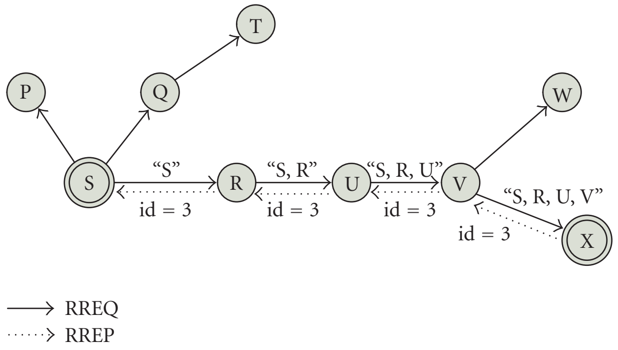

Figure 7: On-demand routing protocol route discovery (S: initiator; X: target).

node S (source or initiator) attempts to discover a route to node X (destination or target). To initiate route discovery, S transmits a route request (RREQ) message as a single local broadcast packet, which is received by all nodes currently within the wireless transmission range of S. Each RREQ message identifies the initiator and target of the route discovery, and contains a unique request id (here, id = 3), determined by the initiator of the request. Each RREQ also contains a record listing the address of each intermediate node through which this particular copy of the RREQ message has been forwarded. This route record is initialized to an empty list by the initiator of the route discovery. When another node receives an RREQ, if it is the target of the route discovery, it returns a route reply (RREP) message to the initiator of the route discovery, giving a copy of the accumulated route record from the RREQ; when the initiator receives this RREP, it caches this route in its route cache for use in sending subsequent packets to this destination. Otherwise, if this node receiving the RREQ has recently seen another RREQ message from this initiator bearing this same request id, or if it finds that its own address is already listed in the route record in the RREQ message, it discards the request. Otherwise, this node appends its own address to the route record in the RREQ message and propagates it by transmitting it as a local broadcast packet (with the same request id).

To return the RREP to the initiator of the route discovery, node X will typically examine its own route cache for a route back to S, and if found, will use it for the source route for delivering the packet containing the RREP. Otherwise, X may perform its own route discovery for target node S; but to avoid possible infinite recursion of route discoveries, it must piggyback this RREP on its own RREQ message for S. Node X could also simply reverse the sequence of hops in the route record that it is trying to send in the RREP, and use this as the source route on the packet carrying the RREP itself. The RREQ contains the following fields:

source_ addr	source_ sequence#	broad-cast_id, dest_addr	dest_ sequence#	hop_ cnt	signal_ strength

The pair ⟨source_addr, broadcast_id⟩ identifies uniquely an RREQ. Broadcast id is incremented whenever the source issues a new RREQ. Each neighbor either satisfies the RREQ by sending a route reply (RREP) back to the source, or rebroadcasts the RREQ to its own neighbors after increasing the hop_cnt. Figure 8 represents the forward path setup as the RREP travels from the destination node D to the source node S. Note that it will timeout after three seconds and will delete the reverse pointers, and that a node may receive multiple copies of the same route broadcast packet from various neighbors. The signal strength has two roles: one as the parameter for selecting destination path and the other as the power strength indicator between vehicle and vehicle or cluster head. When an intermediate node (vehicle or cluster head) receives an RREQ, if it has already received an RREQ with the same broadcast id and source address, it drops the redundant RREQ and does not rebroadcast it. If a node cannot satisfy the RREQ, it keeps track of the following information in order to implement the reverse path setup, as well as the forward path setup that will accompany the transmission of the eventual RREP:

source_ addr	dest_ addr	dest_ sequence#	hop_ cnt	life_ time

A node receiving an RREP propagates the first RREP for a given source node towards that source. If it receives further RREPs, it updates its routing information and propagates the RREP only if the RREP contains either a greater number of destination sequences than the previous RREP, or the same number of destination sequences with a smaller hop count. It suppresses all other RREPs it receives. This decreases the number of RREPs propagating towards the source while also ensuring the most up-to-date and quickest routing information. The source node can begin data transmission as soon as the first RREP is received, and can later update its routing information if it learns of a better route.

Whether rerouting will be performed in advance is decided according to the predictive power value the vehicle received (it denotes the distance or signal strength) from cluster head, the current received power value ($x^{(0)}(k)$) and three historical received values ($x^{(0)}(k-1), x^{(0)}(k-2), x^{(0)}(k-3)$).

To avoid unnecessary calculations of grey prediction, we set a prediction range of 200 m, which is a safe range from the transmitter. Hereafter, the following parameters are defined in the grey prediction algorithm [21, 22].

(1) Power*Received* (k), P_r: signal strength between two communicating nodes. (k represents the relative sequence received from the transmitter or intermediator.)

(2) Receive*Threshold* T_r: signal strength for starting grey prediction (set the start grey prediction for 200 m).

(3) Safe*Threshold* T_s: signal strength for unsafe alarming (set it for 240 m).

(4) Disconnect*Threshold* T_d: signal strength for disconnection range (set the largest transmission for 250 m) [4, 5, 23].

As the other prerouting scheme in [24], Figure 9 demonstrates the preemptive mechanism around a source. For example, when node C moves to Safe*Threshold* 240 m (as node C_4), the grey prediction will initiate to find the vicinal nodes (node D) and the link of communication remains unchanged. When node C_4 moves into range 240–250 m (as node C_n), the signal power of received packets from source node A falls below the Safe*Threshold* (distance greater than 240 m), generating a warning packet to node A. Then, node A initiates route discovery action and can discover fast a new route through node D (because of grey prediction). Hereafter, it switches to this route to avoid failure of the path. Even if node C_n moves out of the radio range of source node A (like node C_m), the new route path still works by forwarding data to node D.

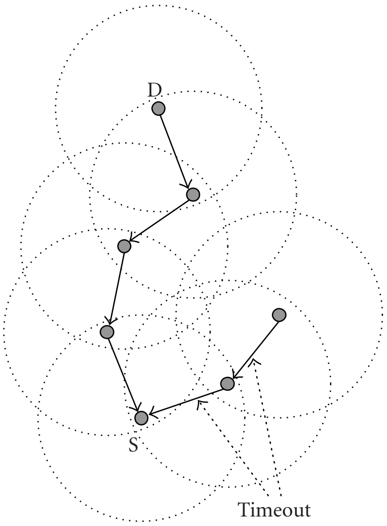

Figure 8: Reverse path formation.

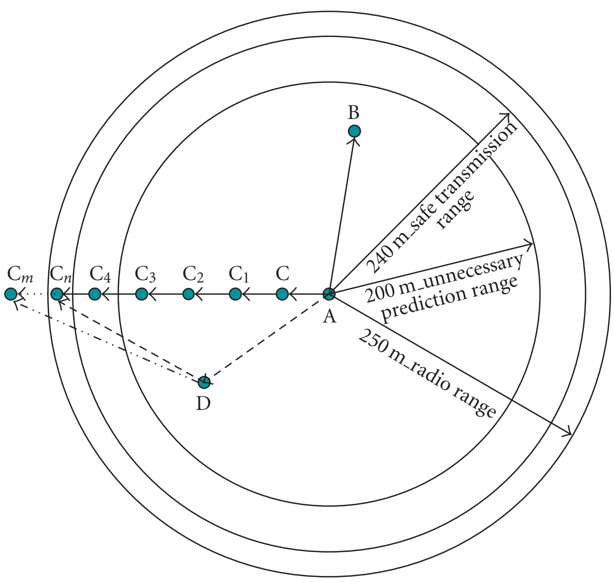
B
240 m_safe transmission range
200 m_unnecessary prediction range
250 m_radio range
C_m
C_n
C_4
C_3
C_2
C_1
C
A
D

Figure 9: Preemptive mechanism and various ranges.

By applying signal strength to GM(1,1), we developed a grey prediction algorithm (Algorithm 1) [21, 22].

Since an explicit estimate of the preemptive range requires the nodes to exchange location and velocity information, we use the signal power [25] of received packets to estimate the distance between them. The recovery time can be related to the power threshold as follows. The signal power drops such that at a distance r from the transmitter, the signal power at any point is the sum of the main signals transmitted by the antenna in addition to components of the signal that reflect off the surrounding features (multipath effect). In an open environment, the main secondary

```
input Power$Received(k)${
    if Power$Received$ $(k) \leqq$ Receive$Threshold$ {            //distance $(k) \geqq 200$ m
        if $(k \geqq 4)${
            generate grey prediction value Power$Received$ $(\hat{x}^{(0)}(k+1))$;
            if Power$Received$ $(\hat{x}^{(0)}(k+1)) <$ Safe$Threshold$ {
                then do $alerting$ and $prerouting$ ;}         //ditance$\geqq$ 240 m
    else k++ ;}
else $x = 0$ ;}        //distance < 200 m does not use grey prediction to reduce load
    }
```

Algorithm 1: Procedure of GTTRR algorithm.

component is the strong reflection of the transmitted signal from the ground. Hence power strength is a value approximated by $P_r = P_0(d/d_0)^{-n_e}$, where P_0 is the power received at the close-in reference point in the far-field region of the antenna at small distance d_0 from the transmitting antenna and n_e is the path loss exponent. Since the energy decay between two nodes is inversely proportional to the distance separating them, we set the path loss exponent n_e to be 4 in our simulation (discussed in Section 3) as follows:

$$P_r = \frac{P_o}{r^n}. \tag{3}$$

We summarize the GTTRR procedure as follows:

(1) making detection,

(2) clustering for energy efficiency [12],

(3) tracking with grey system:

  (3-1) use the k (four historical) data received from the transmitter range value between two communicating nodes to construct a GM(1,1) [13, 26] model,

  (3-2) use the GM(1,1) model to predict $(x^{(0)}(k+1))$. The predicted value is noted as $(\hat{x}^{(0)}(k+1))$,

(4) alerting: if $(\hat{x}^{(0)}(k+1)) \geq T_r$ (T_s is a prerouting Safe*Threshold* at 240 m), broadcast warning message and generate a rerouted call packet broadcast to cluster head or sink,

(5) rerouting: cluster head or sink broadcasts a route request (RREQ) packet to its neighbors and self-heals or reroutes the weak or broken link.

For multicast rerouting of multiple sinks, GTTRR applies the grey prediction system to predict the weak links of multicast trees and reroutes them in advance. If the upper stream path does not fail, it continues to receive data of the multicast tree, until the link breaks or a new path is found. There are two multicasting schemes applied in this paper: MAODV (tree-based) [27] and ODMRP (mesh-based) [23].

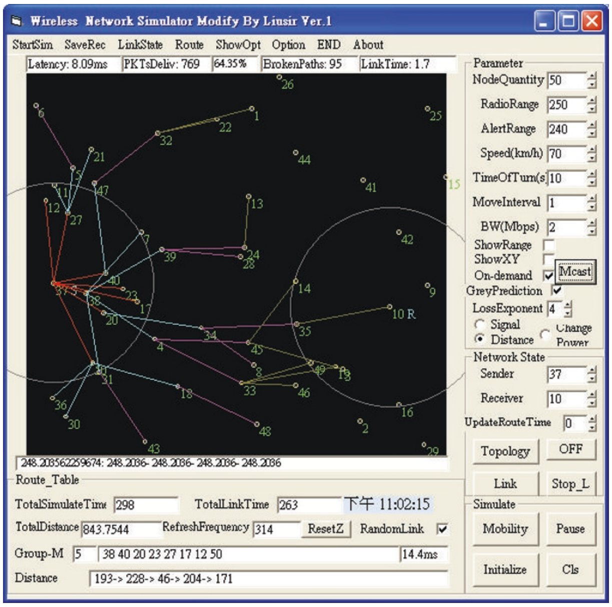

Latency: 8.09ms | PKTsDeliv: 769 | 64.35% | BrokenPaths: 95 | LinkTime: 1.7

Parameter
NodeQuantity 50
RadioRange 250
AlertRange 240
Speed(km/h) 70
TimeOfTurn(s) 10
MoveInterval 1
BW(Mbps) 2
ShowRange □
ShowXY □
On-demand ☑
GreyPrediction ☑
LossExponent 4
○ Signal
● Distance
○ Change Power

Network State
Sender 37
Receiver 10
UpdateRouteTime 0

248.203562259674: 248.2036- 248.2036- 248.2036- 248.2036

Route_Table
TotalSimulateTime 298
TotalLinkTime 263
下午 11:02:15
TotalDistance 843.7544
RefreshFrequency 314
RandomLink ☑
Group-M 5 38 40 20 23 27 17 12 50 14.4ms
Distance 193-> 228-> 46-> 204-> 171

Simulate

Figure 10: Simulations for multicast.

3. SIMULATIONS AND ANALYSIS

In order to verify the characteristics of the proposed schemes, we developed a network model to evaluate rerouting performance on multicast VSN. The simulated screens were shown in Figure 10 [21, 22]. The parameters of the simulation model were assumed as below. Simulation was performed in a square area of 1000 m × 1000 m with 30, 40, and 50 mobile nodes (vehicles). The radio transmission range of vehicle is 250 m [4, 5, 23]. For each ten milliseconds, one of the 10 multicast member groups is randomly changed. The channel traffic is set to be four packets per second [28]. The processing time for receiving and sending out message is three milliseconds (one hop delay time). The working and spare capacities are set to be enough for all calls. The mobility speed is set at the range of 40 km/h to 110 km/h (urban area: 10 m/s; highway: 30 m/s [7]). The total simulation time of each pattern is 1200 seconds. In the simulation, we adopt both MAODV and ODMRP with grey prediction (GTTRR) to compare their efficiencies (we make a summary of the parameters in Table 1).

Figure 11 (50 nodes), Figure 12 (40 nodes), and Figure 13 (30 nodes) show different packet delivery ratios with mobility speeds. Respectively, as speed increases, the routing

Table 1: Simulation parameters.

Parameter	Value
Simulation terrain	1000 m × 1000 m [4, 23]
Simulation time	1200 seconds
Number of nodes (density)	50 [23], 40, and 30 mobile vehicles
Disconnet *Threshold* T_d	Signal strength (dBm) at 250 m [4, 5, 23]
Receive *Threshold* T_r	Signal strength (dBm) at 200 m
Safe *Threshold* T_s	Signal strength (dBm) at 240 m
Vehicular speed range	40 km/h ∼ 110 km/h [7]
Routing protocol	MAODV; ODMRP [23, 27]
Moving direction	Changed by random (9 directions are randomly selected)
Path loss exponent	4
Data-sending rate	4 packets/s [28]

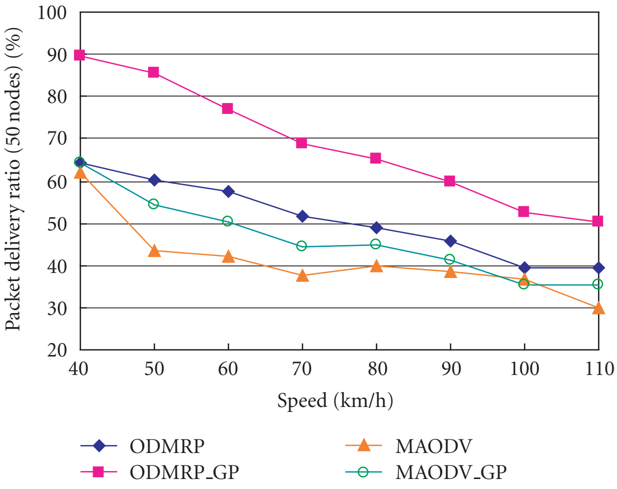

Figure 11: Packet delivery ratio versus mobility speed (50 nodes).

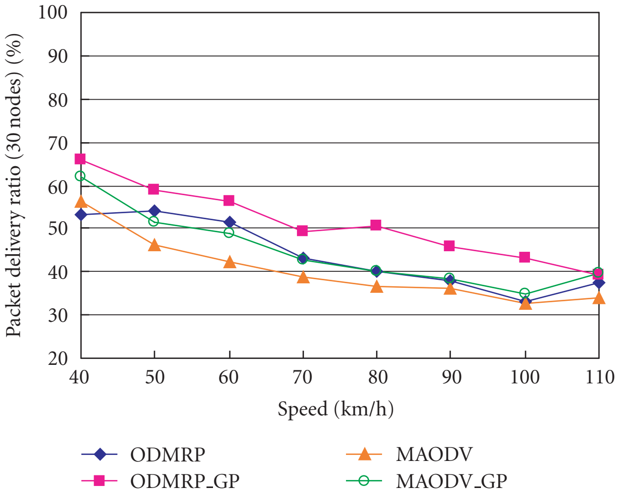

Figure 13: Packet delivery ratio versus mobility speed (30 nodes).

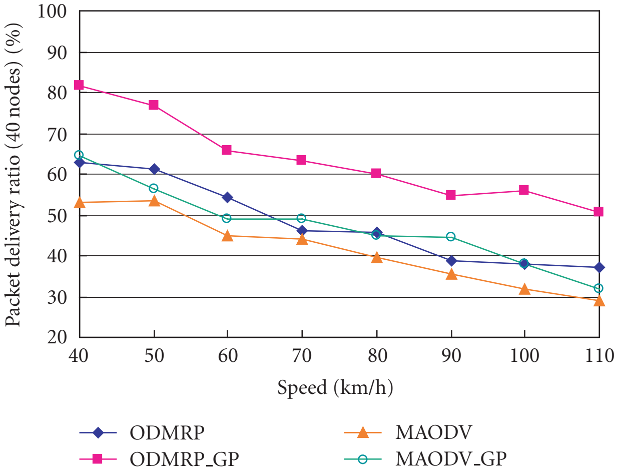

Figure 12: Packet delivery ratio versus mobility speed (40 nodes).

efficiency of the packet delivery ratio degrades rapidly. However, ODMRP-GP has the best performance since there are more redundant routes in the mesh structure. With increasing number of nodes in the topology, the density of the system user dispersion becomes higher. It affects the packet delivery ratio: the larger the number of nodes is, the larger the connection probability it gets. In other words, the packet delivery ratio is proportional to the density of nodes.

Figure 14 (50 nodes), Figure 15 (40 nodes), and Figure 16 (30 nodes) show the average throughput, respectively, as a function of multicast with grey prediction (GP) as speed increases. In this paper, we term throughput as the total amount of packets (data and control packets) transferred from one node (source) to another (receiver) and processed in a specified amount of time. As can be seen, ODMRP has higher throughput, and grey prediction makes the throughput of both multicast schemes better. In this paper, the ODMRP has a set mesh-based topology. As we know, the

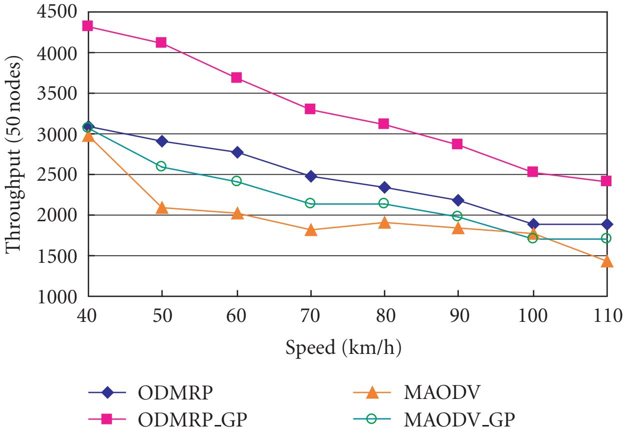

Figure 14: Throughput versus mobility speed (50 nodes).

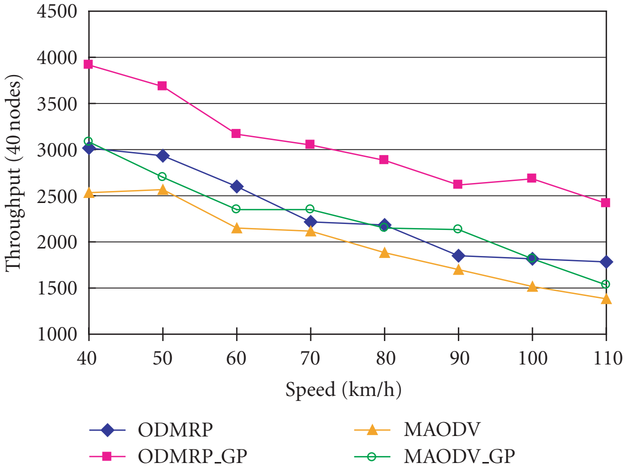

Figure 15: Throughput versus mobility speed (40 nodes).

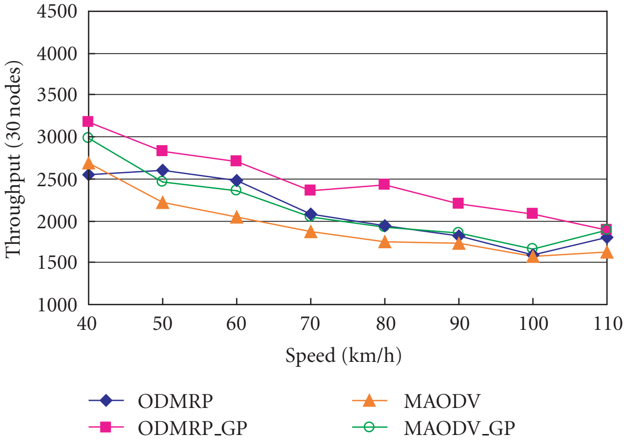

Figure 16: Throughput versus mobility speed (30 nodes).

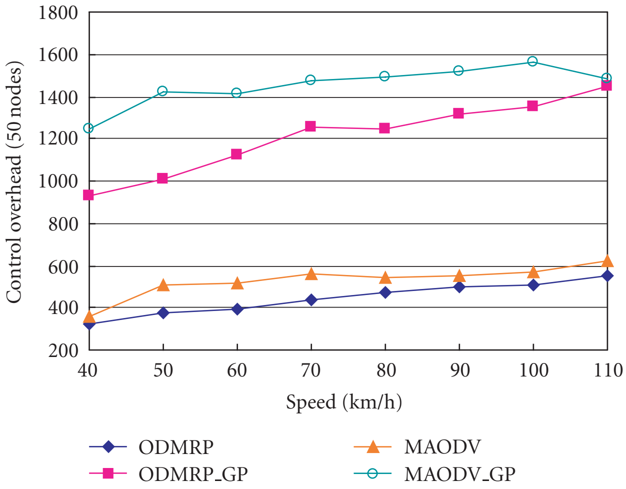

Figure 17: Control overhead versus mobility speed (50 nodes).

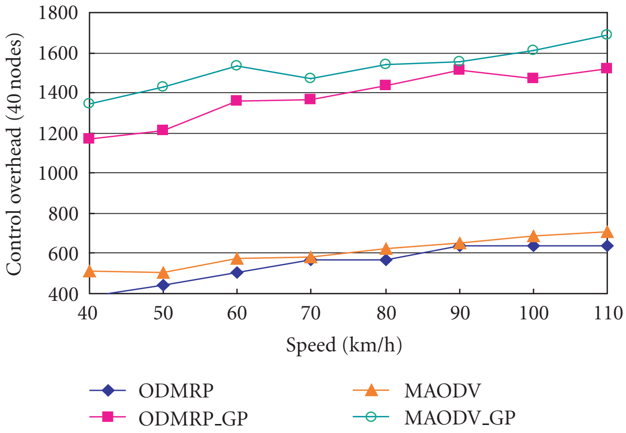

Figure 18: Control overhead versus mobility speed (40 nodes).

mesh conveniently provides alternate paths in failure, thus making better the ODMRP throughput. According to our definitions, the throughput and packet delivery ratio have the same trend. Although ODMRP-GP has the best performance, both MAODV and ODMRP have fewer variations.

Figures 17, 18, and 19 show the control overhead on multicast node densities 50, 40, and 30, respectively. In these three figures, ODMRP has less control overhead than MAODV. One of the reasons is that MAODV has more forward nodes to transmit data and control signals in multicast. Moreover, both MAODV-GP and ODMRP-GP need more control overhead to make the path stable when grey prediction is used. The figure shows if they use grey prediction scheme to improve their data transmission, they need twice above control overheads.

Figures 20, 21, and 22 show the end-to-end delay on multicast node densities 50, 40, and 30, respectively. In multicast, each member does not receive data from the same forwarder; therefore, we calculate the average end-to-end delay

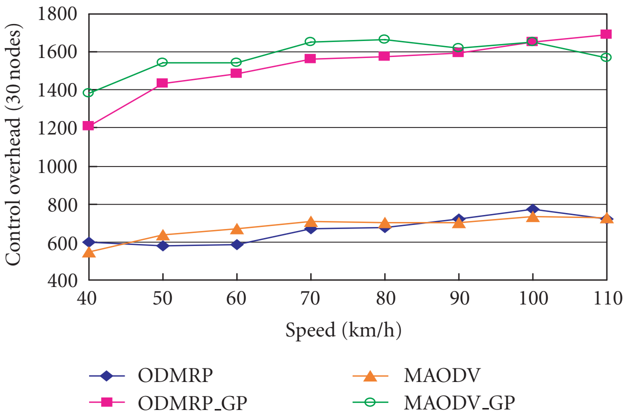

FIGURE 19: Control overhead versus mobility speed (30 nodes).

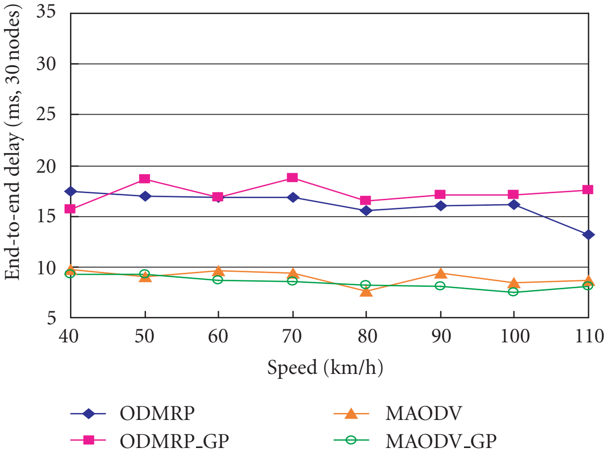

FIGURE 22: End-to-end delay versus mobility speed (30 nodes).

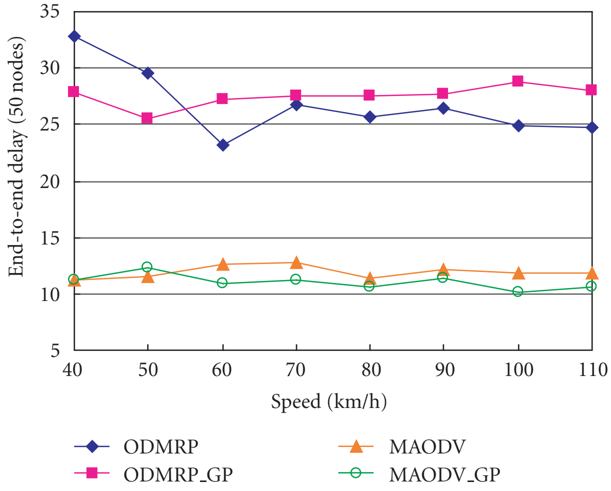

FIGURE 20: End-to-end delay versus mobility speed (50 nodes).

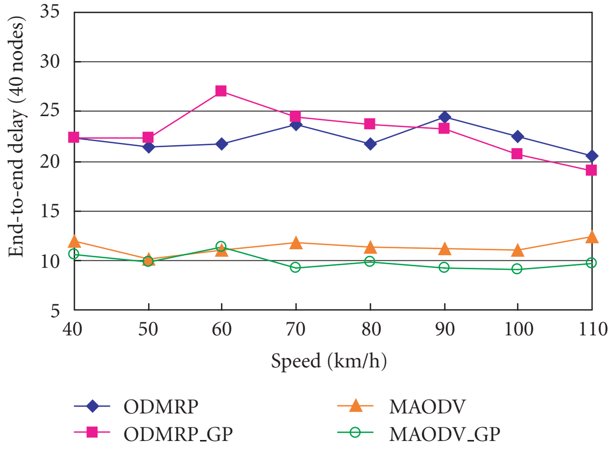

FIGURE 21: End-to-end delay versus mobility speed (40 nodes).

time from the source. In addition, the end-to-end delay of the dropped packets has an infinite delay; hence, we do not include it in the calculation.

As shown in the simulated results, the end-to-end delay did not show obvious difference with increasing mobility speed. Both ODMRP and ODMRP-GP have longer delay time than MAODV and MAODV-GP. However, the number of nodes on the topology is affected seriously. The more the number of nodes is, the more the intermediated nodes are contained. More nodes require more processing time and increase in the end-to-end delay. The higher the node density is, the longer the end-to-end delay is required.

Tables 2, 3, and 4 show the average performance of different node densities versus different routing protocols, respectively. They demonstrate the average performance against packet delivery ratio, throughput, overhead, and end-to-end delay for multicast on VSN. Because combined networks can use multicast trees and meshes to transmit data, the number of broken paths and robustness are not suitable according to the comparison. For packet delivery ratio and throughput on multicast, MAODV-GP and ODMRP-GP are better than MAODV and ODMRP since the prediction mechanism is applied. However, in terms of overhead, MAODV-GP and ODMRP-GP are worse than MAODV and ODMRP. The reason is that the grey system uses more overhead to protect and maintain the communication paths. For end-to-end delay, unfortunately, the grey prediction does not have obvious function to improve their delay.

Finally, for node density, we accumulate the total of the above three tables to find the different performances as integrated in Table 5. The higher the node density is, the more the control overhead is required. Moreover, higher node density means better packet delivery ratio and throughput. On the contrary, the higher the node density is, the longer the end-to-end delay is.

4. CONCLUSION

Wireless VSN has enough processing and storage to handle the data collected before. In traditional static sensor network,

Table 2: Average performances for multicast (50 nodes).

Routing protocol	Packet delivery ratio	Throughput (total)	Control overhead	End-to-end (ms)
MAODV	41.36%	1985.625	528	11.9025
MAODV-GP	46.23%	2219.25	1451	11.02875
ODMRP	50.92%	2444.25	444	26.745
ODMRP-GP	68.56%	3291	1209	27.5125
Total	207.07%	9940.125	3632	77.18875

Table 3: Average performances for multicast (40 nodes).

Routing protocol	Packet delivery ratio	Throughput (total)	Control overhead	End-to-end (ms)
MAODV	41.34%	1984.125	605.125	11.35625
MAODV-GP	47.21%	2266.25	1520.375	9.845
ODMRP	47.96%	2302	547.875	22.31
ODMRP-GP	63.57%	3051.5	1381.125	22.8475
Total	200.08%	9603.875	4054.5	66.35875

sensor data are usually pulled by the sink. When a vehicle moves at a high speed, it will damage the link or cause sink-tree failure. So the activation of the wireless links and such frequent changes in location in the network topology limit transmission range and challenge significantly the survivable operations in the vehicular sensor networks. Therefore, survivable sink multicasting and rerouting in advance becomes an important issue nowadays.

In this paper, we propose a GTTRR scheme to self-heal or reroute weak links before they are broken. Moreover, we expand the traditional multicasting joining both ODMRP and MAODV with grey prediction rerouting in advance to enhance the quality of multicasting wireless onvehicular sensor networks.

For performance evaluation, we simulate multicasting mobile capabilities on two routing schemes: ODMRP and MAODV. MAODV has more multiforwarders than ODMRP. The receivers of multicasting can receive the data from more sources, and MAODV requires more overhead for maintaining the connection paths. Nevertheless, MAODV can support the unicasting at the same time but ODMRP cannot. By selecting suitable parameters and joining with grey prediction, MADOV can obviously decrease the number of broken links and reduce the dissipation of power.

GTTRR on target tracking makes the whole wireless VSN more stable, although it increases average latency and control overhead. However, it supports higher survivability and effective reflections on rerouting.

APPENDIX

A.1. Construction of grey prediction model GM(1,1)

Grey prediction using grey model (GM) involves five operations: accumulated generating operation (AGO), mean operation, grey differential equation modeling, whitening equation for prediction, and inverse accumulated generating operation (IAGO). The GM(1,1) model is the most commonly used model. The first 1 in GM(1,1) means that there is only one variable, and the other 1 means that the first-order grey differential equation is employed to construct the model. The procedure of GM(1,1) model for predicting the value of $x^{(0)}(k+1)$ is described as follows.

Herein, we let $x(0)$ be the nonnegative original data sequence and denote it as

$$x(0) = \left(x^{(0)}(1), x^{(0)}(2), \dots, x^{(0)}(n)\right), \quad \forall n \geq 4, \tag{A.1}$$

where n is the sampling size of the recorded data.

Moreover, the first-order differential grey model GM(1,1) is

$$\frac{dx^{(1)}}{dt} + ax^{(1)} = b, \tag{A.2}$$

where a is the “develop parameter” and b is the “grey input.” The first derivative of AGO sequence $x^{(1)}$ becomes

$$\frac{dx^{(1)}}{dt} = x^{(1)}(k) - x^{(1)}(k-1) = x^{(0)}(k), \tag{A.3}$$

where $k = 2, 3, \dots, n$ and let $z^{(1)}(k)$ be the average of $x^{(1)}(k)$ and $x^{(1)}(k-1)$,

$$Z^{(1)}(k) = 0.5\left[x^{(1)}(k) + x^{(1)}(k-1)\right], \quad k \geq 2. \tag{A.4}$$

In the grey system, we always set factor α to be 0.5; hence, the original intact expression can be shown as

$$Z^{(1)}(k) = \alpha \cdot x^{(1)}(k) + (1-\alpha) \cdot x^{(1)}(k-1), \quad k \geq 2. \tag{A.5}$$

Table 4: Average performances for multicast (30 nodes).

Routing protocol	Packet delivery ratio	Throughput (total)	Control overhead	End-to-end (ms)
MAODV	40.36%	1937.25	678.625	8.9925
MAODV-GP	44.77%	2148.875	1578.375	8.47125
ODMRP	43.89%	2106.5	665.875	16.1425
ODMRP-GP	51.18%	2456.625	1525.5	17.275
Total	180.20%	8649.25	4448.375	50.88125

Table 5: Total value for different nodes density.

Nodes density	Packet delivery ratio	Throughput (total)	Control overhead	End-to-end(ms)
50	207.07%	9940.125	3632	77.18875
40	200.08%	9603.875	4054.5	66.35875
30	180.20%	8649.25	4448.375	50.88125

Next, we approximate the second term of (A.2) and (A.4) and substitute it into (A.3). Then, the first-order grey differential model is established as

$$x^{(0)}(k) + aZ^{(1)}(k) = b, \quad k = 1, 2, 3, \ldots, n,$$
$$x^{(0)}(k) = b - \frac{a}{2}\left[x^{(1)}(k) + x^{(1)}(k-1)\right]. \tag{A.6}$$

The completed grey procedure is as follows.

Step 1. Find the first-order AGO sequence by taking AGO on $x(0)$ and denote it as

$$x^{(1)}(k) = \text{AGO}\left(x^{(0)}(k)\right) = \sum_{i=1}^{k} x^{(0)}(i), \tag{A.7}$$

and the rth-order AGO is defined as

$$x^{(r)}(k) = \sum_{m=1}^{k} x^{(r-1)}(m), \quad k = 1, 2, 3, \ldots, n,$$
$$x^{(r)}(k) = x^{(r)}(k-1) + x^{(r-1)}(k). \tag{A.8}$$

Step 2. As described above, find the background value $Z^{(1)}(k)$ using the mean operation from $x^{(1)}(k)$ and $x^{(1)}(k-1)$,

$$Z^{(1)}(k) = 0.5\left[x^{(1)}(k) + x^{(1)}(k-1)\right], \quad k \geq 2. \tag{A.9}$$

From the background value $Z^{(1)}(k)$, GM(1,1) first-order whitening differential equation can be constructed as

$$\frac{dx^{(1)}(k)}{dk} + aZ^{(1)}(k) = b. \tag{A.10}$$

Step 3. Use least-square method to find matrix B and vector y_n:

$$B = \begin{bmatrix} -Z^{(1)}(2) & 1 \\ -Z^{(1)}(3) & 1 \\ \vdots & \vdots \\ -Z^{(1)}(k) & 1 \end{bmatrix},$$
$$y_n = \left[x^{(0)}(2), x^{(0)}(3), x^{(0)}(4), \ldots, x^{(0)}(n)\right]^T. \tag{A.11}$$

Step 4. Parameters a and b can be obtained by the following operation:

$$\hat{a} = [a, b]^T = \left(B^T B\right)^{-1} B^T y_n, \tag{A.12}$$

where

$$a = \frac{\sum_{k=2}^{n} z^{(1)}(k) \sum_{k=2}^{n} x^{(0)}(k) - (n-1)\sum_{k=2}^{n} z^{(1)}(k) x^{(0)}(k)}{(n-1)\sum_{k=2}^{n}\left[z^{(1)}(k)\right]^2 - \left[\sum_{k=2}^{n} z^{(1)}(k)\right]^2},$$

$$b = \frac{\sum_{k=2}^{n}\left[z^{(1)}(k)\right]^2 \sum_{k=2}^{n} x^{(0)}(k) - \sum_{k=2}^{n} z^{(1)}(k) \sum_{k=2}^{n} z^{(1)}(k) x^{(0)}(k)}{(n-1)\sum_{k=2}^{n}\left[z^{(1)}(k)\right]^2 - \left[\sum_{k=2}^{n} z^{(1)}(k)\right]^2}. \tag{A.13}$$

Step 5. Get the response (whitening) equation

$$\hat{x}^{(1)}(k+1) = \left[x^{(0)}(1) - \frac{b}{a}\right]e^{-ak} + \frac{b}{a}, \quad k = 1, 2, \ldots, n,$$
$$\hat{x}^{(1)}(1) = x^{(0)}(1), \tag{A.14}$$

where $\hat{x}^{(1)}(k+1)$ is the solution of the whitening equation (A.2) or (A.6), and k represents the grey prediction step.

Step 6. Get the forecasting (prediction) value $\hat{x}^{(0)}(k+1)$ by inversing AGO (IAGO) back to the original data sequence:

$$\hat{x}^{(1)}(1) = x^{(0)}(1),$$
$$\hat{x}^{(0)}(k+1) = \hat{x}^{(1)}(k+1) - \hat{x}^{(1)}(k), \quad k = 1, 2, \ldots, n. \tag{A.15}$$

Sometimes (A.15) can be represented by

$$\hat{x}^{(0)}(k+1) = \left(1 - e^{a}\right)\left[x^{(0)}(1) - \frac{b}{a}\right]e^{-ak},$$
$$x^{(1)}(1) = x^{(0)}(1), \tag{A.16}$$

where $\hat{x}^{(0)}(k+1)$ is the prediction result for the next observation.

A.2. An example of MGO

For example, we assume that a data sequence $f(0)$ includes some negative data. We may give a positive reference parameter ε (always set to 1) to adapt the data sequence to nonnegative by bias function. The bias function is denoted as

$$\text{bias} = \left| \min_{k=1}^{n} f^{(0)}(k) \right| + \varepsilon, \qquad \text{(A.17)}$$

and we usually let $\varepsilon = 1$. The MGO operation is expressed as

$$f_m^{(0)} = \text{MGO} \circ f^{(0)} = f^{(0)} + \text{bias}. \qquad \text{(A.18)}$$

Example 1. If we have a sequence $f(0) = \{-1, -2, 1, 2\}$, we can get the bias by (A.17),

$$\text{bias} = \left| \min_{k=1}^{n} f^{(0)}(k) \right| + \varepsilon = |-2| + 1 = 3, \qquad \text{(A.19)}$$

and we can transfer the nonnegative sequence by MGO operation:

$$f_m^{(0)} = \text{MGO} \circ f^{(0)} = f^{(0)} + \text{bias} = \{2, 1, 4, 5\}. \qquad \text{(A.20)}$$

If the MGO operation is executed, the inverse operation (IMGO) must be used and it is necessary to correct the predicted value. The inverse operation (IMGO) is as follows:

$$\hat{f}^{(0)} = \text{IMGO} \circ \hat{f}_m^{(0)} = \hat{f}_m^{(0)} - \text{bias}, \qquad \text{(A.21)}$$

where $\hat{f}$ means that its value is predicted by grey prediction.

REFERENCES

[1] B. Liu, P. Brass, O. Dousse, P. Nain, and D. Towsley, "Mobility improves coverage of sensor networks," in *Proceedings of the 6th ACM International Symposium on Mobile Ad Hoc Networking and Computing (MobiHoc '05)*, pp. 300–308, Urbana-Champaign, Ill, USA, May 2005.

[2] I. F. Akyildiz, W. Su, Y. Sankarasubramaniam, and E. Cayirci, "A survey on sensor networks," *IEEE Communications Magazine*, vol. 40, no. 8, pp. 102–114, 2002.

[3] D. Niculescu, "Communication paradigms for sensor networks," *IEEE Communications Magazine*, vol. 43, no. 3, pp. 116–122, 2005.

[4] H. Alshaer and E. Horlait, "An optimized adaptive broadcast scheme for inter-vehicle communication," in *Proceedings of the 61st IEEE Vehicular Technology Conference (VTC '05)*, vol. 5, pp. 2840–2844, Stockholm, Sweden, May-June 2005.

[5] U. Lee, E. Magistretti, B. Zhou, M. Gerla, P. Bellavista, and A. Corradi, "MobEyes: smart mobs for urban monitoring with vehicular sensor networks," Tech. Rep. 060015, UCLA CSD, Los Angeles, Calif, USA, 2006.

[6] M. Durresi, A. Durresi, and L. Barolli, "Sensor inter-vehicle communication for safer highways," in *Proceedings of the 19th International Conference on Advanced Information Networking and Applications (AINA '05)*, vol. 2, pp. 599–604, Taipei, Taiwan, March 2005.

[7] H. Saito, "Performance analysis of combined vehicular communication," *IEICE Transactions on Communications*, vol. E89-B, no. 5, pp. 1486–1494, 2006.

[8] H. C. Chang, H. Du, J. Anda, C.-N. Chuah, D. Ghosal, and H. M. Zhang, "Enabling energy demand response with vehicular mesh networks," in *Proceedings of the 6th IFIP IEEE International Conference on Mobile and Wireless Communication Networks (MWCN '04)*, pp. 371–382, Paris, France, October 2004.

[9] C.-C. Wong, B.-C. Lin, and C.-T. Cheng, "Fuzzy tracking method with a switching grey prediction for mobile robot," in *Proceedings of the 10th IEEE International Conference on Fuzzy Systems*, vol. 1, pp. 103–106, Melbourne, Australia, December 2001.

[10] R. C. Luo and T. M. Chen, "Target tracking by grey prediction theory and look-ahead fuzzy logic control," in *Proceedings of IEEE International Conference on Robotics and Automation*, vol. 2, pp. 1176–1181, Detroit, Mich, USA, May 1999.

[11] C. E. Perkins and E. M. Royer, "Ad-hoc on-demand distance vector routing," in *Proceedings of the 2nd IEEE Workshop on Mobile Computing Systems and Applications (WMCSA '99)*, pp. 90–100, New Orleans, La, USA, February 1999.

[12] S. D. Muruganathan, D. C. F. Ma, R. I. Bhasin, and A. O. Fapojuwo, "A centralized energy-efficient routing protocol for wireless sensor networks," *IEEE Radio Communications Magazine*, vol. 43, no. 3, pp. 8–13, 2005.

[13] J. Deng, *Essential Topics on Grey System: Theory and Application*, China Ocean Press, Beijing, China, 1988.

[14] X. Wu, H. Heo, R. A. Shaikh, J. Cho, O. Chae, and S. Lee, "Individual contour extraction for robust wide area target tracking in visual sensor networks," in *Proceedings of the 9th IEEE International Symposium on Object and Component-Oriented Real-Time Distributed Computing (ISORC '06)*, pp. 179–185, Gyeongju, South Korea, April 2006.

[15] R. C. Luo, T. M. Chen, and K. L. Su, "Target tracking using hierarchical grey-fuzzy motion decision-making method," *IEEE Transactions on Systems, Man, and Cybernetics—Part A*, vol. 31, no. 3, pp. 179–186, 2001.

[16] I. Pavlidis and N. P. Papanikolopoulos, "Automatic selection of control points for deformable-model-based target tracking," in *Proceedings IEEE International Conference on Robotics and Automation*, vol. 4, pp. 2915–2920, Minneapolis, Minn, USA, April 1996.

[17] E. M. Royer and C. K. Toh, "A review of current routing protocols for ad hoc mobile wireless networks," *IEEE Personal Communications*, vol. 6, no. 2, pp. 46–55, 1999.

[18] R. Gupta and S. R. Das, "Tracking moving targets in a smart sensor network," in *Proceedings of the 58th IEEE Vehicular Technology Conference (VTC '03)*, vol. 5, pp. 3035–3039, Orlando, Fla, USA, October 2003.

[19] K. Sanzgiri, I. D. Chakeres, and E. M. Belding-Royer, "Pre-reply probe and route request tail: approaches for calculation of intra-flow contention in multihop wireless networks," *Mobile Networks and Applications*, vol. 11, no. 1, pp. 21–35, 2006.

[20] D. B. Johnson, D. A. Maltz, and J. Broch, "DSR: the dynamic source routing protocol for multi-hop wireless ad hoc networks," in *Ad Hoc Networking*, chapter 5, pp. 139–172, Addison-Wesley, Reading, Mass, USA, 2001.

[21] Y.-F. Wang and L.-L. Liu, "Grey-based prerouting and target tracking on vehicular sensor networks," in *Proceedings of the National Symposium on Telecommunications (NST '06)*, Kaohsiung, Taiwan, December 2006.

[22] Y.-F. Wang and L.-L. Liu, "Grey target tracking on vehicular sensor networks," in *Proceedings of International Conference on Late Advances in Networks (ICLAN '06)*, Paris, France, December 2006.

[23] S.-J. Lee, W. Su, and M. Gerla, "On-demand multicast routing protocol in multihop wireless mobile networks," *Mobile Networks and Applications*, vol. 7, no. 6, pp. 441–453, 2002.

[24] T. Goff, N. B. Abu-Ghazaleh, D. S. Phatak, and R. Kahvecioglu, "Preemptive routing in ad hoc networks," in *Proceedings of the 7th Annual International Conference on Mobile Computing and Networking (MOBICOM '01)*, pp. 43–52, Rome, Italy, July 2001.

[25] S. L. Su, Y. C. Su, and J. F. Huang, "Grey-based power control for DS-CDMA cellular mobile systems," *IEEE Transactions on Vehicular Technology*, vol. 49, no. 6, pp. 2081–2088, 2000.

[26] X. Wang and X. Wu, "Application of grey system models to rural economy analysis in China," in *Proceedings of the 1st International Conference on Uncertainty Modelling and Analysis*, pp. 511–516, College Park, Md, USA, December 1990.

[27] E. M. Royer and C. E. Perkins, "Multicast Ad Hoc on Demand Distance Vector (MAODV) routing," *IETF Internet draft*, draft-ietf-manet-maodv-00.txt, 2000.

[28] L. Qin and T. Kunz, "Pro-active route maintenance in DSR," *ACM SIGMOBILE Mobile Computing and Communications Review*, vol. 6, no. 3, pp. 79–89, 2002.